Water Stability of Sulfonated Polyimide Membranes

Yan Yin,[†] Yoshiki Suto,[‡] Takaaki Sakabe,[‡] Shouwen Chen,[‡] Shunsuke Hayashi,[‡] Takashi Mishima,[‡] Otoo Yamada,[†] Kazuhiro Tanaka,[‡] Hidetoshi Kita,[‡] and Ken-ichi Okamoto*[,‡]

Venture Business Laboratory, Yamaguchi University, Ube, Yamaguchi 755-8611, Japan, and Department of Advanced Materials Science & Engineering, Faculty of Engineering, Yamaguchi University, Tokiwadai 2-16-1, Ube, Yamaguchi 755-8611, Japan

Received November 8, 2005; Revised Manuscript Received December 12, 2005

ABSTRACT: The water stability of sulfonated copolyimides (SPIs) derived from 1,4,5,8-naphthalenetetracarboxylic dianhydride (NTDA), sulfonated diamines of 4,4′-bis(4-aminophenoxy)biphenyl-3,3′-disulfonic acid (*p*BAPBDS), and 2,2′- or 3,3′-bis(3-sulfopropoxy)benzidine (2,2′- or 3,3′-BSPB) and nonsulfonated diamines was investigated in detail from viewpoints of viscosity, mechanical strength, proton conductivity, weight loss, and hydrolysis products eluted into the soaking water. With the aging in water or 100% relative humidity vapor at 130 °C, the polymer chain scission took place mainly in the early stage but thereafter slightly, and as a result the SPI membranes kept the reasonably high mechanical properties even after 192 h. The branched/cross-linked SPI membranes prepared by incorporating a flexible triamine kept better mechanical properties. The weight loss and sulfur loss of <10% were observed for the *p*BAPBDS-based SPIs. This was due mainly to the elution of hydrolysis product, the oligomer of NTDA, and sulfonated diamine, which did not contain the nonsulfonated diamine moieties. With the aging at 130 °C, the proton conductivity did not change for the *p*BAPBDS-based SPIs, but for the BSPB-based SPIs it decreased 20% in water and much more at the lower relative humidities because of the cleavage of the sulfopropoxy group. The accelerated water stability tests reveal that the water stability of the present SPI membranes is not sufficiently high at 130 °C but is high enough for PEFC and DMFC applications at least at 80 °C.

Introduction

Recently, there has been much interest in the development of polymer electrolyte fuel cells (PEFCs) having high performance, high durability, and potentially lower cost for transportation and stationary and portable power applications.[1,2] Polymer electrolyte membrane (PEM) is one of the key components of a PEFC system. Perfluorosulfonic acid copolymer membranes, such as DuPont's Nafion membrane, are the state-of-the-art PEMs because of their high proton conductivity and excellent chemical stability.[3,4] However, because of their high cost, low operational temperature below 80 °C, and large methanol crossover, there has been much interest in alternative PEMs. Many efforts have been done in the development of PEMs based on sulfonated aromatic hydrocarbon polymers.[5−9]

Sulfonated naphthalenic polyimides with six-membered imide rings have been reported to be promising candidates for PEFCs. Mercier and co-workers developed sulfonated block copolyimides from 1,4,5,8-naphthalenetetracarboxylic dianhydride (NTDA), 2,2′-benzidinedisulfonic acid (BDSA), and common nonsulfonated diamines.[10−14] The sulfonated block copolyimide membranes have been reported to show reasonably high performance in a H_2/O_2 fuel cell system at 60 °C for more than 3000 h. However, the proton conductivities of these membranes were rather lower due to their lower ion exchange capacity (IEC) values, which were essential for maintaining membrane durability toward water. This seems to limit the further improvement in PEFC performance.[14]

We synthesized novel sulfonated (co)polyimides (SPIs) from NTDA, novel different sulfonated diamines, and nonsulfonated diamines, of which the chemical structures are shown in Figure 1, and investigated the relationship between the chemical structure and water stability of the SPI membranes.[15−20] The water stability was evaluated by the elapsed time until the membrane hydrated in water lost the mechanical property. The loss of mechanical property was judged when the membrane broke after being lightly bent in the case of the soaking at 80 °C or when the membrane began to break into pieces under boiling in the case of soaking at 100 °C.[18] The data are summarized in Table 1. The water uptake (*WU*) shown in Table 1 was calculated from the weights of dry (W_d) and water-swollen (W_s) membranes as follows:

$$WU = (W_s - W_d)/W_d \times 100\% \quad (1)$$

The water stability was a result of the total effect of solubility stability, hydrolysis stability, and swelling-stress stability. The solubility stability was mainly determined by the IEC and the configuration of the sulfonated diamine moiety. The high IEC and nonlinear configuration led to poor solubility stability and vice versa. The hydrolysis stability of the imide ring was strongly dependent on the basicity of the sulfonated diamine moiety. Highly basic diamines gave much better hydrolysis stability than weakly basic ones. We classified the sulfonated diamines into two groups. The sulfonated diamines such as BDSA and 4,4′-diaminodiphenyl ether-2,2′-disulfonic acid (ODADS), where the electron-withdrawing sulfonic acid groups are bonded directly to the aminophenyl rings, are noted as "type 1". On the other hand, "type 2" diamines developed, where the sulfonic acid groups are bonded to aromatic rings other than the aminophenyl rings, are 4,4′-bis(4-aminophenoxy)biphenyl-3,3′-disulfonic acid (*p*BAPBDS), 2,2′-bis(4-aminophenoxy)-biphenyl-5,5′-disulfonic acid (*o*BAPBDS), 9,9-bis(4-aminophenyl)fluorene-2,7-disulfonic acid (BAPFDS), and bis[4-(4-

[†] Venture Business Laboratory.
[‡] Department of Advanced Materials Science & Engineering.
* Corresponding author: Tel 0836-85-9660; Fax 0836-85-9601; e-mail okamotok@yamaguchi-u.ac.jp.

10.1021/ma0523769 CCC: $33.50
Published on Web 01/12/2006

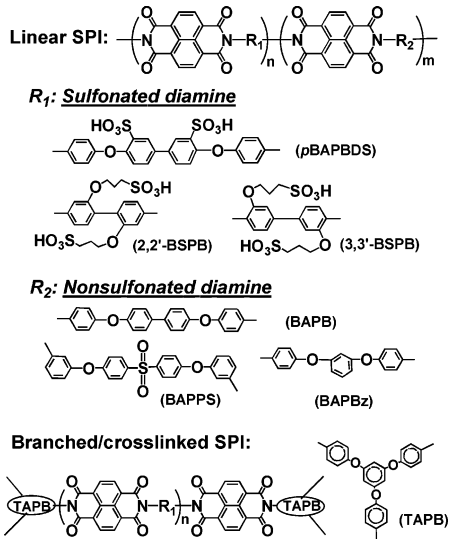

Figure 1. Chemical structure of NTDA-based SPIs.

Table 1. IEC, WU, and Water Stability of NTDA-Based SPIs

SPIs	IEC[a] (mequiv/g)	WU[b] (wt %)	water stability T (°C)	water stability time (h)	ref
BDSA/ODA (1/1)	1.98	79	80	5	16
BDSA/BAPBz (1/1)	1.82	77,[c] 68[d]	80	60	this
BDSA/DDS (1/1)	1.66	21	80	110	25
ODADS/ODA (1/1)	1.95	87	80	25	15
ODADS/BAPB (1/1)	1.68	57	80	200	15
BAPFDS/ODA (1/1)	1.71	78	80	26	16
*o*BAPBDS/BAPB (2/1)	1.89	152	80	105	19
*p*BAPBDS/BAPB (2/1)	1.89	63	100	>1000	18
*p*BAPBDS/BAPBz (2/1)	1.96	70,[c] 58[e]	100	>500	this
*p*BAPPSDS/BAPPS (2/1)	1.73	98[c]	100	>200	20
*m*BAPPSDS/BAPS (3/7)	1.59	53[d]	80	42	30
DAPPS	2.09	105[d]	80	200	31
2,2′-BSPB	2.89	220[d]	100	2500	32
3,3′-BSPB	2.89	250[d]	100	700	32
2,2′-BSPB/BAPB (2/1)	2.02	61[e]	100	>3000	33
3,3′-BSPB/BAPB (2/1)	2.02	64[e]	100	>3000	33
*p*BAPBDS/TAPB (6/1)	2.29	77[e]	100	>3000	35

[a] Calculated value. [b] At 80 °C. [c] At 100 °C. [d] At 50 °C. [e] At 30 °C.

aminophenoxy)phenyl]sulfone-3,3′-disulfonic acid (*p*BAPPSDS). The type 2 diamines are more basic than the type 1 diamines and as a result have the higher hydrolysis stability. The flexible structure due to flexible linkage such as ether bond enables easy molecular relaxation of polymer chain under membrane swelling to reduce swelling stress, resulting in the better water stability. As shown in Table 1, the *p*BAPBDS-based SPIs with linear configuration, higher basicity, and more flexible structure displayed much better water stability than the SPIs based on other sulfonated diamines.

Other research groups have reported on synthesis and proton conductivity of BDSA-based copolyimides with different nonsulfonated diamine moieties. Miyatake et al. have reported on high proton conductivities more than 0.2 S/cm at 100% relative humidity (RH) and high temperatures above 100 °C for their BDSA-based SPI membranes, whereas they did not mention the water stability.[21−24] Lee et al. have reported on the water stability up to 110 h at 80 °C for their BDSA-based SPI membranes.[25,26] Recently, the research group of Mercier and Diat et al. has reported on the aging of the BDSA-based block copolyimide membranes in PEFCs and in hot water.[27,28] The predominant aging mechanism was imide group hydrolysis, which was significantly accelerated above 80 °C. These results lead us to the view that a series of copolyimide membranes derived from NTDA, BDSA, and different nonsulfonated diamines generally have poor water stability at temperatures above 80 °C unless a special and significant improvement is achieved.

McGrath et al. have reported on novel co-SPIs based on bis[4-(3-aminophenoxy)phenyl]sulfone-3,3′-disulfonic acid (*m*BAPPSDS).[29,30] As listed in Table 1, the *m*BAPPSDS-based co-SPIs displayed the rather poor water stability. The NTDA-*m*BAPPSDS/BAPPS(3/2) membrane became brittle after soaking in water for 42 h at 80 °C. The intrinsic viscosity decreased from an original value of 2.51 dL/g down to 0.38 dL/g after the soaking, indicating hydrolytic chain scission.

The above-mentioned SPIs are the main-chain-type ones, where the sulfonic acid groups are bonded directly to aromatic rings composing polymer chains. We also synthesized side-chain-type SPIs bearing pendant sulfoalkoxy groups, of which the chemical structures are shown in Figure 1, and investigated the water stability of their membranes.[31−33] The data are also summarized in Table 1. The SPIs based on 2,2′-bis(3-sulfopropoxy)benzidine (2,2′-BSPB) and 3,3′-bis(3-sulfopropoxy)-benzidine (3,3′-BSPB) displayed much better water stability than the main-chain-type SPIs. This may partly come from the higher basicity of the diamine moieties due to the electron-donating effect of propoxy groups. Furthermore, the microphase-separated structure also plays an important role in their high water stability. Asano et al. also reported on the excellent hydrolytic stability of 3,3′-BSPB-based co-SPIs.[34]

Branched/cross-linked sulfonated polyimide (B/C-SPI) membranes, of which the chemical structure is also shown in Figure 1, were prepared by incorporating 1,3,5-tris(4-aminophenoxy)-benzene (TAPB), a triamine with flexible ether linkages, into the polymer chain.[35] The B/C-SPI membranes had a network structure and were not soluble in any solvents and as a result displayed much better water stability than the corresponding linear SPI membranes, as listed in Table 1.

The higher operational temperature enables the achievement of the higher overall efficiency of a PEFC. So, alternative PEMs must be operational at higher temperatures than at least 80 °C and favorably 100 °C. Among the SPI membranes mentioned above, the linear- and B/C-SPIs based on *p*BAPBDS, 2,2′-BSPB, and 3,3′-BSPB have high potential as such high-temperature PEMs. In this paper, the water stability of these SPI membranes is investigated in detail from different viewpoints.

Experimental Section

Sample Preparation. Co-SPIs were prepared from NTDA, sulfonated diamines (*p*BAPBDS, 2,2′-BSPB, and 3,3′-BSPB), and nonsulfonated diamines via statistical or sequenced polycondensation reactions in *m*-cresol according to the methods previously reported.[18,33] Nonsulfonated diamines used are 4,4′-bis(4-aminophenoxy)biphenyl (BAPB), bis[4-(3-aminophenoxy)phenyl] sulfone (BAPPS), and 1,3-bis(4-aminophenoxy)benzene (BAPBz). Membranes were prepared by casting their *m*-cresol solution (5−10 wt %) onto glass plates and dried at 120 °C for 10 h. The as-cast membranes were soaked in methanol at room temperature for 48 h to remove the residual solvent, followed by the proton exchange treatment in 1 M sulfuric acid at 50 °C for 2−5 days. The proton-exchanged membranes were washed with water for 2 days and then cured in vacuo at 150 °C for 10 h or 150 °C for 1 h and then 200 °C for 1 h. For example, the abbreviation of NTDA-*p*BAPBDS/BAPB(2/1) refers to statistical (or random) copolyimide of NTDA with *p*BAPBDS and BAPB with a feed molar ratio of 2/1. The abbreviation including "-s" at the end refers to sequenced block copolyimide.

Table 2. Physical Properties of NTDA-Based SPI Membranes

code no.	SPIs	IEC[a] (mequiv/g)	$[\eta]$[b] (dL/g)	*WU*[c] (wt %)	size change Δt_c	size change Δl_c	T_{d1} (°C)
M1	*p*BAPBDS	2.63	1.73	115[d]	0.32	0.087	
M2-1	*p*BAPBDS/BAPB (2/1)	1.89 (1.86)	1.03	80	0.37	0.063	
M2-2	*p*BAPBDS/BAPB (2/1)	1.89 (2.0)	2.7	51	0.20	0.044	
M2-3	*p*BAPBDS/BAPB (2/1)	1.89	4.4	57	0.14	0.049	
M3-1	*p*BAPBDS/BAPBz (2/1)	1.96	(4.9)	58 (70[e])	0.10	0.070	309
M3-2	*p*BAPBDS/BAPBz (2/1)	1.96	(7.7)	53	0.14	0.065	
M3-3	*p*BAPBDS/BAPBz (2/1)	1.96	(2.0)	55	0.14	0.070	
M4	*p*BAPBDS/BAPPS (3/2)-s	1.66	1.83	48	0.15	0.047	309
M5	BDSA/BAPBz (1/1)	1.82	(3.3)	68 (77[e])	0.20	0.03	
M6-1	2,2′-BSPB/BAPB (2/1)	2.02		76[d]	0.49	0.047	232
M6-2	2,2′-BSPB/BAPB (2/1)	2.02	4.5	72	0.47	0.043	248
M7	2,2′-BSPB/BAPB (2/1)-s	2.02		87	0.55	0.045	255
M8	2,2′-BSPB/BAPPS (2/1)	1.95		39[d]	0.10	0.023	254
M9-1	3,3′-BSPB/BAPB (2/1)	2.02 (1.72)		62[d]	0.48	0.030	
M9-2	3,3′-BSPB/BAPB (2/1)	2.02 (1.73)	5.7	64	0.39	0.034	252
M10	*p*BAPBDS/TAPB (6/1)	2.29 (2.32)		77	0.23	0.077	
M11	*p*BAPBDS/TAPB (6/1) (chemical imidization)	2.29		62	0.27	0.032	
M12	2,2′-BSPB/TAPB (7.5/1)	2.57		104	0.59	0.012	256
M13	3,3′-BSPB/TAPB (7.5/1)	2.57		134	1.28	0.017	

[a] Calculated values, the data in parentheses are measured values by titration. [b] Intrinsic viscosity at 35 °C, the data in parentheses are reduced viscosity measured at 0.5 g/dL in *m*-cresol. [c] At 30 °C. [d] At 50 °C. [e] At 100 °C.

B/C-SPIs were prepared by a one-pot two-step method.[35] First, the anhydride-terminated SPI oligomers were prepared from NTDA and sulfonated diamine in *m*-cresol in the presence of triethylamine (TEA) and benzoic acid at 180 °C for 20 h. The molar ratio of NTDA over sulfonated diamine was controlled to be 5/4 or 6/5. TAPB was then added into the oligomer solution as a branching and cross-linking reactant. The reaction mixture was heated to 50 °C for 2−5 h until the viscosity of the solution became reasonably high, at which stage the solution was cast onto glass plates at 50 °C in an oven. The oven temperature was raised slowly to 120 °C and maintained for 10 h. The membranes were heated under vacuum at 200 °C for 10 h for thermal imidization, followed by soaking in methanol and proton exchange as mentioned above. Some membranes were soaked in a mixture of acetic anhydride and pyridine (1/1, v/v) at 50 °C for 2 days for chemical imidization, followed by the same posttreatment mentioned above. For example, the abbreviation of NTDA-*p*BAPBDS/TAPB(6/1) refers to copolyimide of NTDA and *p*BAPBDS branched/cross-linked with TAPB, where a feed molar ratio of NTDA/*p*BAPBDS/TAPB is 7.5/6/1.

Measurements. Thermogravimetry−mass spectrometry (TG−MS) was performed on a (Shimadzu) MS−(Rigaku) TG/8120 in helium (flow rate: 100 cm^3/min) at a heating rate of 5 °C/min. Mechanical tensile tests were performed on an universal testing machine (Orientic, TENSILON RTC-1150A) at 25 °C and around 60% RH. UV−vis absorption spectra were recorded on an UV/vis spectrophotometer (Jasco, V-550). IR absorption spectra were recorded on a FT/IR-610 (Jasco) spectrometer from solution-cast films. ^{1}H NMR spectra were recorded on a JEOL EX270 (270 MHz) instrument. ICP emission spectrography was performed on an ICP emission spectrophotometer (Perkin-Elmer, Optima 4300DV). Ion chromatography was performed on ionchromatograph (Dionex, DX-320) with a MS (Agilent Technologies, 1100 Series LC/MSD SL).

Proton conductivity σ in plane direction of membrane was determined using an electrochemical impedance spectroscopy technique over the frequency range from 10 Hz to 100 kHz (Hioki 3532-80) as reported in the literature.[18,33] Water uptake of the fully hydrated SPIs was measured by immersing membrane samples (100−200 mg) into water at a given temperature for 3−5 h. Then the samples were taken out, wiped with tissue paper swiftly, and weighed on a microbalance. The dimensional change of the SPI membranes was measured by immersing the round-shaped samples into water at room temperature for 3−5 h; the changes of thickness and diameter, Δt_c and Δl_c, respectively, were calculated as reported in the literature.[18,33] Viscosity measurements were carried out for *m*-cresol solutions of SPI in TEA salt form in the concentration range of 1.0−0.2 g/dL at 35 °C with an Ostwald-type viscometer. The intrinsic viscosity $[\eta]$ was determined by combined use of the Huggins plot, Fuoss−Mead plot, and Billmeyer plot.

Water Stability Test. Water stability tests were carried out by aging membrane sheets (150−200 mg) of SPIs in proton form under the following three different test conditions, namely, (1) in water (100 mL) at 100 °C for 48−300 h, (2) in water (90 mL) at 130 °C under pressure for 24−196 h, and (3) in water vapor phase (50 mL) equilibrated with water (50 mL in 100 mL pressure vessel) at 130 °C under pressure (hereafter abbreviated to "in 100% RH vapor at 130 °C") for 24−96 h. After being kept under a test condition, the membrane sheets were dried under vacuum at 120 °C for 3 h and then subjected to the characterization experiments including mechanical property, proton conductivity, and so on. The mechanical property was evaluated by tensile strength (Young's modulus, maximum stress, and elongation at break) and membrane toughness by the bending test. The bending test was carried out for a membrane sheet 5 mm in wide and 20 mm in length at room temperature and around 60% RH. The membrane toughness level was set as follows. In level I, the membrane is brittle and breaks into pieces by handling. In level II, the membrane sheet breaks when it is bent by holding both ends between fingers. In level III, the membrane sheet breaks along a fold when it is folded to zero degree. In level IV, the membrane sheet breaks when it is folded back. In level V, the membrane sheet does not break after it is folded back.

The soaking water solutions were also subjected to the instrumental analysis including UV spectroscopy, ICP emission spectrography, ion chromatography, and so on. In the case of the test in 100% RH vapor at 130 °C, before drying, the membrane sheets were soaked in water at 30 °C for 2 days. Both water samples were subjected to the analysis. Trace amounts of sulfur in sample water solutions were determined by the ICP analysis using data at an emission wavelength of 181.975 nm.

The FT-IR spectra and ^{1}H NMR spectra were measured for the residue on distillation of soaking water solution. For this purpose, membrane sample of 500 mg was soaked in 100 mL of water at 130 °C.

Results and Discussion

The physical properties of NTDA-based SPI membranes used in this study are listed in Table 2. **M2**−**M4** and **M6**−**M9** are linear co-SPIs from *p*BAPBDS and 2,2′- or 3,3′-BSPB, respectively. **M5** is a linear co-SPI from BDSA, which was used for comparison. **M10**−**M11** and **M12**−**M13** are B/C-SPIs from *p*BAPBDS and 2,2′- or 3,3′-BSPB, respectively. The results of

Table 3. Properties of NTDA-Based SPI Membranes before and after Aging in Water at 100 °C

code no.	soaking time (h)	weight loss (%)	S loss (mol %)	naphthalenic loss (mol %)	σ (50 °C, mS/cm) in water	90%	70%	50%RH	*YM* (GPa)	*MS* (MPa)	*EB* (%)	tough-ness
M2-1	0				140	89	28	2.5	1.6	85	80	V
	96	0.5	1.7	2.3					1.4	37	8	V
	192		1.7		131	91	28	2.8				V
	300	2.0	2.9	3.0					1.6	40	4	IV
M2-3	0								1.8	120	120	V
	300	2.8	1.7	7.3					1.6	49	8	V
M3-2	0								1.6	81	90	V
	96	0.1	1.3	2.0					1.4	45	6	V
	300	5.2	3.2	4.8					1.4	47	6	V
M6-1	0				138	99	9.1	1.0				V
	48		22		96	80	4.4	0.07				V
	300		21		113	93	1.4	0.05				IV
M6-2	0				154[a]	95[a]	15.4[a]	2.8[a]	2.1	127	86	V
	48	2.2	11	2.9	130[a]	75[a]	7.8[a]	1.2[a]	2.3	68	12	V
	200	9.6	17	7.3	146[a]	80[a]	9.6[a]	1.5[a]	1.7	57	6	IV
M7	0				113	101	8.0	0.85				V
	48		3.0		98	90	16	1.6				V
	300		5.0		93	90	11					V
M8	0				47	18	3.9	0.04				V
	48		4.0		54	24	3.5	0.03				V
	300		6.0		46	29	2.6	0.05				V
M9-1	0				121[a]	116[a]	23[a]	2.3[a]				V
	48		13		104[a]	114[a]	19[a]	1.7[a]				V
	300		11		118[a]	109[a]	9.1[a]	1.2[a]				IV
M9-2	0				135[a]	107[a]	16[a]	1.6[a]	1.9	172	84	V
	48	4.1	22	0	99[a]	49[a]	6.9[a]	0.64[a]	1.9	113	41	V
	300	6.1	22	5.0	99[a]	53[a]	7.0[a]	0.61[a]				IV

[a] Measured at 60 °C.

Table 4. Properties of NTDA-Based SPI Membranes before and after Aging in Water at 130 °C

code no.	soaking time (h)	weight loss (%)	S loss (mol %)	naphthalenic loss (mol %)	σ (50 °C, mS/cm) in water	90%	70%	50%RH	*YM* (GPa)	*MS* (MPa)	*EB* (%)	tough-ness
M2-2	0				117	94	18	2.3	1.2	100	120	V
	24	8.3	1.8		94	86	16	2.0	0.80	44	6	V
	48	7.6	4.0		91	86	16	2.1	0.81	40	6	V
	96	7.0	6.5						0.61	34	6	V
M3-2	0								1.3	64	95	V
	24	3.6	7.5	6.6					1.3	33	6	V
	96	10	12	11.6					1.1	30	6	V
M3-3	0				102[b]		13[b]	2.3[b]	1.4	81	95	V
	192[a]	7.3	8.1	8.1	103[b]		13[b]	2.9[b]	1.2	55	10	V
M4	0				91[b]	77[b]	19[b]	3.2[b]	1.2	78	94	V
	48	0.3	1.0		91[b]	75[b]	20[b]	4.0[b]	1.2	67	11	V
	48−96	7.0	2.6		87[b]	72[b]	16[b]	3.5[b]	1.1	62	12	V
M5	0								2.6	85	50	V
	24	37	46	41		not measurable				not measurable		I
	24[a]	NM	44	53								
M10	0				148	84	16	2.7	1.2	98	110	V
	48	6.6	5.7	−	142	98	17	2.4	0.90	55	10	V
	96	8.3	7.9	−	136	94	22	3.2	0.88	54	13	V
M11	0				122	83	17	3.5	0.97	97	130	V
	48	3.7	4.8		120	83	17	3.9	0.91	50	13	V
	96	8.2	6.2		113	82	19	3.8	0.89	49	15	V
	192	9.4	7.2		114	89	18	4.0	0.91	48	14	V
M12	0				150	95	12	1.7				V
	48	15				90	4.4	0.14	2.4	120	9	V
	96	13				67	1.7		2.3	83	5	V
M13	0				147	128	11	1.1	2.3	120	18	V
	48	11	22		100	125	6.1	0.44	2.0	120	16	V
	96	10	22		91	109	6.1	0.34	1.93	110	17	V
	196	18	30		118		3.6	0.10	2.0	90	12	V

[a] Performed with large amout of sample of over 0.5 g. [b] At 60 °C.

water stability tests under the three different conditions are summarized in Tables 3−5.

Intrinsic Viscosity. Molecular weight changes with the water stability tests are essential information about the hydrolytic stability of polymer chains of SPIs. GPC measurements could not be done because the SPIs did not dissolve in a proper solvent such as NMP. The SPIs in TEA salt form dissolved in *m*-cresol, but those in proton form did not. So, for the viscosity measurements, the SPI membranes in proton form used in the water stability tests had to be changed to the TEA salt form. The sample sheets were put in water in a beaker, and a 0.1 wt % TEA solution was added very slowly, with keeping the pH of water solution less than 8.5. However, with this ion-exchange procedure, the base-catalyzed hydrolysis of polymer chain took place to a certain extent, resulting in an appreciable decrease in $[\eta]$. This was serious for the SPIs with higher viscosity (or

Table 5. Properties of NTDA-Based SPI Membranes before and after Aging in 100% RH Vapor at 130 °C

code no.	time (h)	weight loss (%)	S loss (mol %)	naphthalenic loss (mol %)	σ (60 °C, mS/cm) in water	90%	70%	50% RH	*YM* (GPa)	*MS* (MPa)	*EB* (%)	tough-ness
M3-2	0								1.3	64	95	V
	24	1.9	3.2	0.2								V
	96	3.0	3.3	0.3					1.2	34	5	V
M6-2	0				154	95	15.4	2.8	2.1	127	86	V
	48	7.9	14	0.7					2.2	32	3	V
	96	9.4	15	1.2	123	49	6.2	0.39	2.1	33	3	IV

higher molecular weight). For example, in the case of **M6-2**, the [η] values decreased by 60% from its original value of 4.5 dL/g down to 1.8 dL/g after the ion-exchange procedure. Therefore, we did not measure viscosity change with the water stability tests, except for the following cases.

Figure 2 shows variation in [η] with soaking time in water at 100 °C for **M1** (homo-SPI) and **M2-1** (co-SPI with lower viscosity). In the case of **M1** and **M2-1**, the reduction in [η] with the ion-exchanging procedure was rather small, namely, 15% and 25% from their original values of 1.73 and 1.03 dL/g down to 1.47 and 0.77 dL/g, respectively. So, in evaluation of the data in Figure 2, we should take into account that the actual [η] values of the soaked membranes might be to some extent larger than the observed values.

As shown in Figure 2, for **M1**, the [η] decreased down to a third of the original value after the soaking at 100 °C for 24 h, but did not further decrease after 50 h. The initial decrease in [η] was smaller for **M2-2**, although its initial [η] was as low as 0.8 dL/g, and it kept a fairly high [η] value of 0.5 dL/g even after 300 h. This indicates that the polymer chain scission due to the hydrolysis of imide ring occurred in the initial period of the soaking but very slowly in the further soaking, and the molecular weight might be kept at a reasonable level for further prolonged soaking at 100 °C. This may be the reason that the BAPBDS-based SPI membranes kept their sheet-shape in boiling water for more than 1000 h as mentioned above.

These results suggest the presence of some parts being less stable against the hydrolytic scission in polymer chains than other parts. Hydrolytic polymer chain scission seems to take place fast there in the early stage and then slowly in other parts.

According to the paper by McGrath et al., NTDA-*m*BAPPSDS/BAPPS(3/2) membrane became brittle after soaking in water for 42 h at 80 °C followed by the significant decrease in intrinsic viscosity from an original value of 2.51 dL/g down to 0.38 dL/g.[30] On the other hand, the para-isomer, NTDA-*p*BAPPSDS/BAPPS(2/1) membrane, has been reported to display much better water stability of more than 200 h at 100 °C,[20] as listed in Table 1. The para-isomer in proton form did not dissolve in solvents, and the viscosity change with the aging was not measured. The *p*BAPBDS-based SPIs, the para-isomer in the present study, also displayed much better water stability and smaller reduction in [η]. It seems reasonable to consider that the para-isomers give better water stability than the meta-isomers, although further study is necessary.

Mechanical Properties. The mechanical property stability of SPI membrane is an important factor affecting membrane performance. The mechanical properties were evaluated by means of tensile strength and membrane toughness.

The typical stress−strain curves of SPI membranes before and after aging in water at 100 °C are shown in Figure 3. The unaged sample displayed a large elongation after a yield point until a break point, whereas the aged sample displayed a much smaller elongation. As a result, the aged sample showed smaller maximum stress and much smaller elongation degree at break point compared to the unaged one, although Young's modulus was not so different between them. As can be seen from Table 3, such a change in the tensile strength property took place mainly in the initial period (48−96 h) of the soaking and the further soaking until 300 h slightly reduced the tensile strength property. This behavior is similar to the viscosity change with the soaking time mentioned above. So, after soaking for 300 h, the *p*BAPBDS-, 2,2′-BSPB-, and 3,3′-BSPB-based SPI membranes still kept reasonably high Young's modulus and maximum stress more than 1 GPa and 40 MPa, respectively, and also fairly high membrane toughness level of V or IV.

As shown in Table 4, in the case of aging in water at 130 °C, the similar change in the tensile strength property took place within 24 h, and the further soaking very slightly reduced the tensile strength property. Comparison among **M2-2**, **M3-2**, **M3-3**, and **M4** shows that the tensile strength property was similar before the aging but after the aging was slightly better for **M3-3** and **M4** than for the others. This might be due to some effect of nonsulfonated diamine structure and/or polymer segment structure as well as small difference in membrane morphology between different preparation batches. After soaking for 96 or 192 h, these *p*BAPBDS-based SPI membranes still kept reasonably high Young's modulus and maximum stress more than 0.6 GPa and 30 MPa, respectively, and also high membrane toughness level of V. On the other hand, the BDSA-based SPI membrane (**M5**) is noted to completely loose its mechanical strength after soaking for 24 h, indicating much poorer hydrolytic stability than the *p*BAPBDS-based SPIs.

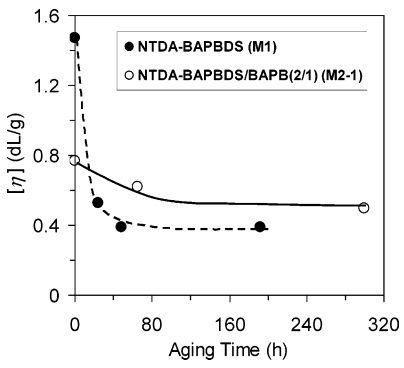

Figure 2. Variation in [η] of SPIs with aging in water at 100 °C.

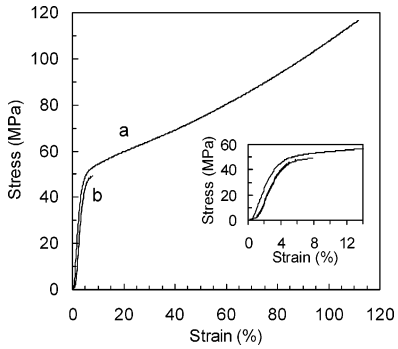

Figure 3. Stress−strain curves of **M2-3** (a) before and (b) after aging in water at 100 °C for 300 h.

The B/C-SPI membranes, **M10** to **M13**, showed much better water stability from the viewpoint of mechanical property than the linear SPI membranes. After aging in water at 130 °C for 192 h, **M11** showed Young's modulus, maximum stress, and elongation degree at break point of 0.9 GPa, 50 MPa, and 14%, respectively. The corresponding values for **M13** were 2.0 GPa, 90 MPa, and 12%. The network structure was effective to keep the mechanical strength at high level as possible as for long soaking time.

As can be seen from Table 5, the change in the mechanical properties with the aging in 100% RH vapor at 130 °C was similar to that with the aging in water at the same temperature.

As mentioned above, the commonly observed behavior with the aging in water or saturated vapor at high temperatures was a significant decrease in large elongation after a yield point until a break point and the corresponding reduction in maximum stress, which was due to the reduced effect of polymer chain entanglement as a result of polymer chain scission. This took place mainly in the early period of the aging and further reduction in the tensile strength properties with the prolonged aging was rather small, and most of the SPI membranes, especially for the B/C-SPI ones, kept their mechanical properties at a reasonably high level.

Weight Loss and Spectroscopic Analysis. Weight loss (wt %) was calculated from the difference between weights of a membrane sample before and after the aging, and its experimental error was about ±1.5 wt %. Sulfur loss (mol %) is the ratio of sulfur atom amount dissolved into water with the aging test, which was determined by the ICP analysis, over the original sulfur amount in membrane (calculated value), and its experimental error was about ±2 mol %. These data are listed in Tables 3−5. With some exceptions, both weight loss and S loss increased with an increase in aging time and also with an increase in aging temperature. In the case of *p*BAPBDS-based SPI membranes (**M2**−**M4**, **M10**, and **M11**), the weight loss and S loss with aging in water at 100 °C for 300 h were as small as 2−5 wt % and 2−3 mol %, respectively, whereas they became as large as 7−10 wt % and 4−9 mol %, respectively, at 130 °C for 96−192 h. The latter values were not so small. On the other hand, the BDSA-based SPI membrane (**M5**) displayed extremely large weight loss and S loss of 37 wt % and 46 mol %, respectively, at 130 °C for only 24 h and broke into pieces.

In the case of 2,2′-(or 3,3′)-BSPB-based SPI membranes (**M6**−**M9**, **M12**, and **M13**), both weight loss and S loss were larger compared with the *p*BAPBDS-based SPIs. With the aging at 100 °C, the S loss significantly varied from membrane to membrane; that is, it was much smaller for **M7** and **M8** than for **M6-1** and **M9-2**. Pairs of **M6-1** and **M6-2**, and also of **M9-1** and **M9-2**, of which the chemical structure is the same and only the preparation batch was different, displayed significantly different S loss values.

The aging in 100% RH vapor at 130 °C gave much smaller weight and S losses than the aging in water for the *p*BAPBDS-based SPI membranes. For the BSPB-based SPI membranes, although there is no data for direct comparison, the similar behavior was reasonably deduced from the data of Tables 3−5.

The FT-IR spectra of *p*BAPBDS- and BSPB-based membranes were compared between before and after the aging in water. Typical examples are shown in Figure 4. There was observed no appreciable change except for appearance of very weak peak of acid carbonyl at 1786 cm^{-1} after the aging. However, the acid carbonyl peak was much smaller than the imide carbonyl peak at 1712 cm^{-1}. For example, the peak

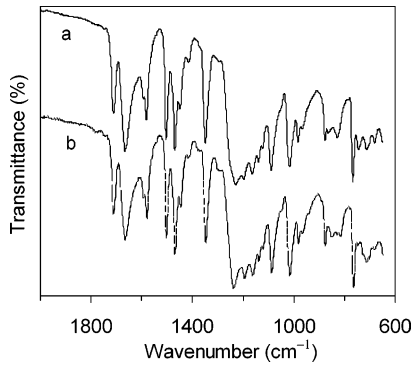

Figure 4. FTIR spectra of **M3** (a) before and (b) after aging in water at 130 °C for 192 h.

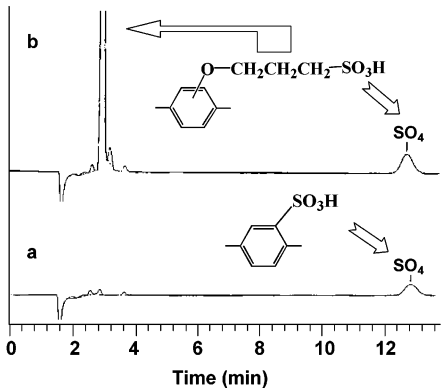

Figure 5. Anion chromatograph spectra of soaking water solutions after aging (a) **M2-2** and (b) **M13** in water at 130 °C for 48 h.

intensity ratio of 1786 cm^{-1} over 1712 cm^{-1} was 1/30 for **M2-1** with the aging at 100 °C for 300 h and 1/20 for **M4** and **M12** at 130 °C for 96 h. Furthermore, the intensity ratio hardly changed with an increase in aging time from 48 h up to 96 or 192 h. This indicates the hydrolysis of imide ring into acid and amino groups took place to some extent in the initial period of the aging but very slowly in the further aging.

Figure 5 shows anion chromatograph spectra of soaking water solutions after aging **M2-2** and **M13** membranes in water at 130 °C for 48 h. The elution peaks around 13 min were attributed to SO_4^{2-} ion produced by hydrolysis of sulfonic acid group. The decomposition degree of sulfonic acid group was calculated as the ratio of the amount of SO_4^{2-} ion observed in soaking water over the original SO_3H amount in membrane (calculated value). The decomposition degrees of sulfonic acid group were 0.36 and 0.49 mol % at 130 °C for 24 and 96 h, respectively, for **M2-2** and 0.55 and 0.65 mol % at 130 °C for 48 and 196 h, respectively, for **M13**. The small decomposition degree and its small increase with an increase in soaking time indicate the reasonably high hydrolysis stability of sulfonic acid for the *p*BAPBDS- and BSPB-based SPIs. In the case of **M13**, a large peak appeared at an elution time of 3 min. The ion chromatograph/MS analysis showed the *m*/*z* value of this peak was 139, which was in agreement with that of $[HO(CH_2)_3SO_3]^-$. The authentic sample of 3-hydroxypropanesulfonic acid gave the same result, whereas the reference sample of propanesulfonic acid gave another peak with *m*/*z* of 123. This indicated that the cleavage of ether bond of sulfopropoxy group took place fairly easily at 130 °C for the BSPB-based SPIs.

Figure 6 shows UV spectra of soaking water solutions after the aging of SPI membranes in water at 100 and 130 °C. For comparison, the UV spectra of NTDA-based SPIs, 1,4,5,8-naphthalenetetracarboxylic acid (NTCA), and BAPBDS and

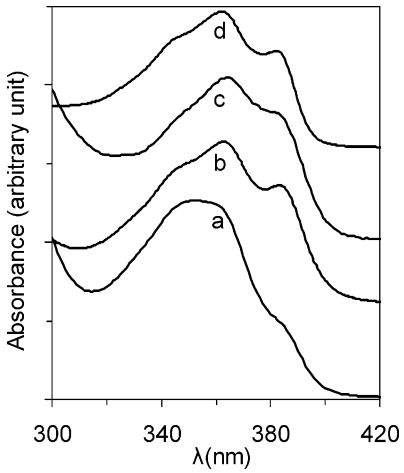

Figure 6. UV spectra of soaking water solutions after the aging of SPI membranes: (a) **M2-3** at 100 °C for 300 h, (b) **M6-2** at 100 °C for 200 h, (c) **M3-3** at 130 °C for 192 h, and (d) **M5** at 130 °C for 24 h.

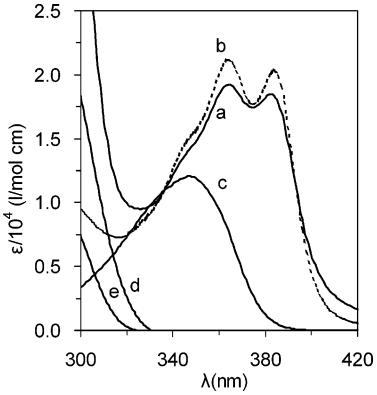

Figure 7. UV spectra of NTDA-based SPIs in *m*-cresol/DMSO/water (1/7/8, v/v) solution, naphthalenetetracarboxylic acid (NTCA), and sulfonated diamines in water: (a) **M2**, (b) **M8**, (c) NTCA at pH 3.8, (d) BAPBDS, and (e) 2,2′-BSPB.

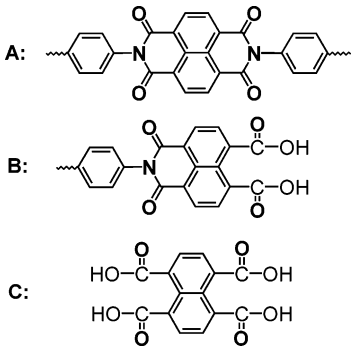

Figure 8. Chemical structure of naphthalenic components produced by the hydrolysis.

2,2′-BSPB are shown in Figure 7. The absorption bands of 320−420 nm are attributed to the naphthalenic components. The absorption bands of the NTDA-based SPIs, which resemble each other, have two peaks at 385 and 364 nm and one shoulder around 340 nm. This means that these absorption bands are attributed to the naphthalenic imide−imide structure (**A** in Figure 8) and the substitution of phenylene unit of diamine hardly affects the absorption band. On the other hand, NTCA at pH 3.8 shows a broad absorption band with a peak at 348 nm. The absorption bands in Figure 6 are attributed to naphthalenic components in the soaking water solutions, which were considered to be composed of structures **A**, **B,** and **C**, as shown in Figure 8. At present, we have no data of absorption spectrum of the imide−acid structure **B** component. To a first approximation, we assumed that the imide−acid structure component had a similar absorption band to the imide−imide structure component and had almost the same extinction coefficient as the other components (**A** and **C**) at 340 nm. On this assumption, the concentrations of the total naphthalenic components (**A** + **B** + **C**) in the soaking water solutions were evaluated using the extinction coefficient of 1.20×10^4 L/(mol cm) and the absorbance data at 340 nm. Using these values, the naphthalenic component losses (mol %) with the aging were calculated and listed in Tables 3−5. The naphthalenic component loss was closely correlated to the weight loss as for the aging in water, whereas it was much smaller for the aging in 100% RH vapor.

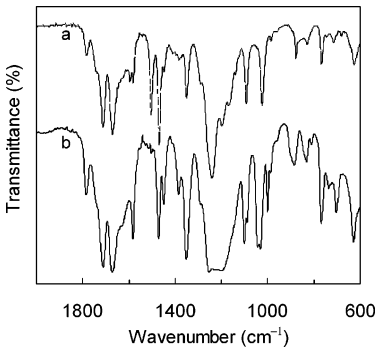

Figure 9. FT-IR spectra of the residue on distillation of soaking water solutions for (a) **M3-3** and (b) **M5** in KBr.

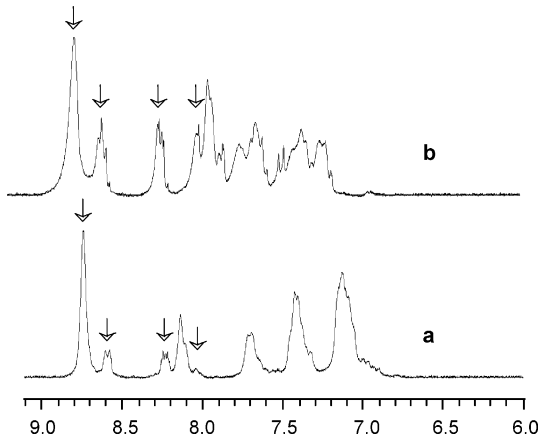

Figure 10. ^{1}H NMR spectra of the residue on distillation of soaking water solutions for (a) **M3-3** and (b) **M5** in DMSO-d_6.

The FT-IR spectra and ^{1}H NMR spectra were measured for the residue on distillation of soaking water solutions for **M3-3** and **M5**, as noted by superscript "*a*" in Table 4. The FT-IR spectra are shown in Figure 9. They showed imide carbonyl (1712, 1668 cm^{-1}), acid carbonyl (1784 cm^{-1}), naphthalenic C=C (1581 cm^{-1}), imide C−N (1348 cm^{-1}), and O=S=O of sulfonic acid (around 1020 cm^{-1}). The ^{1}H NMR spectra are shown in Figure 10. On the hydrolysis study of a naphthalenic imide model compound, Mercier et al. reported that the hydrolysis product of the imide−acid structure (**B** in Figure 8) showed two doublets at 8.22 and 8.57 ppm.[36] They also reported that naphthalenic protons of NTCA and NTDA showed singlet peaks at 8.03 and 8.71 ppm, respectively. They also demonstrated that the naphthalenic protons of copolyimide from NTDA, BDSA, and 1,4-bis(4-aminophenoxy)-2-*tert*-butylbenzene showed a doublet peak at 8.74−8.78 ppm.[13] The naphthalenic protons of NTDA-based co-SPIs (in TEA salt form)

Table 6. Ratios of Naphthalenic Components and Sulfonated Diamine Residue Dissolving out in the Soaking Water during the Aging of SPI Membranes at 130 °C for 192 h (M3-3) and 24 h (M5)

code no.	naphthalenic components[a] A	B	C	sulfonated diamine/ naphthalenic
M3-3	1.00	0.32	0.04	0.86
M5	1.00	0.67	0.30	1.05

[a] A, B, and C are shown in Figure 8.

dissolved in DMSO have been reported to show a doublet-like peak at 8.7−8.8 ppm.[13,29] Therefore, the singlet peak at 8.75 and 8.80 ppm for **M3-3** and **M5**, respectively, in Figure 10 was attributed to equivalent naphthalenic protons of the imide−imide structure (**A** in Figure 8). The chemical shift was slightly larger for **M5** than for **M3-3** because of the electron-withdrawing effect of sulfonic acid group on the aminophenylene unit in BDSA moiety. The peaks at 8.58−8.64, 8.22−8.28, and 8.03 ppm in Figure 10 were attributed to naphthalenic protons of *imide*−acid, imide−*acid*, and acid−acid structures, respectively. The naphthalenic component ratio was evaluated from the peak ratios and is summarized in Table 6. The protons of 2-, 4-, and 5-positions of the central phenylene ring of BAPBz appear at 6.3−6.5 ppm. However, there was no peak in the range of 6.0−6.9 ppm in Figure 10, indicating no presence of BAPBz component in the residue of the soaking water. Therefore, the other peaks in the range of 7.0−8.2 ppm in Figure 10 were attributed to phenylene protons of BAPBDS and BDSA components. The ratio of sulfonated diamine component per naphthalenic one dissolved out into the soaking water was evaluated as 0.86 and 1.05 for **M3-3** and **M5**, respectively.

As can be seen in Figure 6, the absorption peaks at 385 and 364 nm attributed to the imide−imide structure were clearer for **M5** than for **M3-3**, indicating the higher ratio of imide−imide structure component over the other components for **M5**. This was different from the results from the ^{1}H NMR spectra listed in Table 6. This is probably because further hydrolysis of imide−imide structure component to imide−acid and acid−acid structure components took place for **M3-3** during the concentration of the soaking water under vacuum at 70 °C for 2 h.

The ^{1}H NMR spectra also showed a triplet at 1.3 ppm and a quartet at 3.2 ppm, which were attributed to methyl and methylene protons, respectively, of triethylamine. This indicates some amount of triethylammonium sulfate still remained in membranes after the proton exchange and soaking in water and dissolved into water during the aging.

The above-mentioned results and discussion lead us to the following conclusions about the hydrolysis. (1) With the aging in water at 130 °C, the polymer chain scission took place via the hydrolysis mainly on the imide (and/or isoimide and amide acid, if present) bonds neighboring sulfonated diamine residues but hardly on the bonds neighboring nonsulfonated diamine residues. (2) The hydrolysis took place much more easily for the BDSA-based SPIs than for the *p*BAPBDS- and BSPB-based SPIs. (3) The component dissolved out in the soaking water was composed mainly of oligomers of NTDA and sulfonated diamine. Judging from the low ratios of imide−acid and acid−acid structure, the presence of an insoluble part in the concentrated water solution, and appreciable viscosity of the concentrated DMSO solution, the oligomers are considered to have two or three repeat units of imide−imide structure and one or two imide−acid structure at the chain end(s). (4) With the aging in 100% RH vapor at 130 °C, the polymer chain scission took place in the similar degree compared with the aging in water, judging from the similar change in mechanical properties, although the weight loss, S loss, and naphthalenic loss in water were much lower. This was because the major hydrolysis product or the oligomers hardly dissolved out into water by soaking at 30 °C for 2 days. The weight loss and S loss were fairly larger for the BSPB-based SPIs than the *p*BAPBDS-based SPIs because the sulfopropoxy groups, another hydrolysis product, easily dissolved out into water by the soaking.

Proton Conductivity. Proton conductivity stability of SPI membrane is also another important factor affecting membrane performance. In the case of *p*BAPBDS-based SPI membranes, no appreciable change in proton conductivity with aging was observed in the whole range of relative humidity even after the aging in water at 100 °C for 300 h and in water or 100% RH vapor at 130 °C for 96−192 h, although the weight loss and sulfur loss up to 10 wt % and 9 mol %, respectively, took place. As shown in Table 4, for example, **M3-3** displayed σ values at 60 °C of 102 mS cm^{-1} in water and 2.3 mS cm^{-1} at 50% RH, which had little difference from those of 103 and 2.9 mS cm^{-1}, respectively, after aging in water at 130 °C for 192 h. This is probably because the sulfonic acid content in membrane after the aging might not decrease so large as the sulfur loss. Thus, the *p*BAPBDS-based SPI membranes showed the high proton conductivity stability.

On the other hand, in the case of 2,2′-(or 3,3′)-BSPB-based SPI membranes, the proton conductivities decreased with the aging at 130 °C. The decrease in σ significantly depended on the relative humidity. As shown in Table 4, after aging **M13** for 196 h, the reduction in σ from 147 to 118 mS cm^{-1} in water was only 20% and rather small, but with decreasing RH the reduction in σ increased significantly up to 85−90% at 50% RH (from 1.1 to 0.1 mS cm^{-1}). Table 5 also shows the decrease in σ from 154 to 123 mS cm^{-1} in water (by 20%) and from 2.8 to 0.39 mS cm^{-1} at 50% RH (by 86%), for **M6-2** after aging in 100% RH vapor at 130 °C for 96 h. As mentioned above, a large part of the sulfur loss was due to the cleavage of sulfopropoxy group rather than the hydrolysis of the imido ring followed by dissolution of the sulfonated diamine residue, resulting in an appreciable decrease in the sulfonic acid content in membrane. The actual decrease in IEC might be not so large and affect slightly the conductivity in water but more largely at lower RH. With the aging at 100 °C, as mentioned above, the S loss significantly varied from membrane to membrane, and the proton conductivity change also varied similarly. For **M7** and **M8**, of which the sulfur losses were smaller, no appreciable change in σ was observed in the whole range of RH even after the aging for 300 h. On the other hand, for **M6-1** and **M9-2**, of which the sulfur losses were larger, the larger decrease in σ took place at the lower RHs (see Table 3), as in the case of the aging at 130 °C. Thus, the BSPB-based SPI membranes displayed rather poor proton conductivity stability, especially with the aging at 130 °C. With the aging at 100 °C, some membranes showed reasonably high proton conductivity stability. The BSPB-based SPI membranes have the microphase-separated structure,[33] and rather small difference in membrane morphology might play a large role in their proton conductivity stability.

From the viewpoints of mechanical stability, hydrolytic stability, and proton conductivity stability, BAPBDS-based B/C-SPI and some linear SPI membranes displayed the water stability of 192 h for the accelerated test at 130 °C and were reasonably considered to have the water stability as long as 300 h or more, judging from the variation in the mechanical properties with

the aging time. Assuming the activation energy of hydrolytic degradation of 100 kJ/mol,[28] the water stability of 300 h at 130 °C corresponds to 3300, 8000, 20 000, and 160 000 h at 100, 90, 80, and 60 °C, respectively. Taking the operational humidity condition of 70−80% RH in PEFC application, their water stability would be much more improved. Therefore, BAPBDS-based SPI membranes have the reasonably high water stability and high potential for PEFC application at 80 °C and also at 90−100 °C with further improvement. We have performed the short-term durability test for a PEFC with NTDA-BAPBDS/BAPB(2/1), which kept the cell voltage of 0.77 V for more than 300 h under a constant current density of 0.5 A/cm^2, a cell temperature of 90 °C, humidifier temperatures of anode and cathode of 85 and 82 °C, respectively, and a gas pressure of 0.3 MPa for H_2 and O_2.[37] The PEFC application of BSPB-based SPI membranes may be limited below 80 °C because of the hydrolytic stability of the sulfopropoxy group. Both BAPBDS- and BSPB-based SPI membranes have no problem as for the water stability for DMFC applications below 60 °C.

Conclusions

(1) For the *p*BAPBDS-based SPIs, the large decrease in $[\eta]$ and large decrease in tensile strength, especially elongation degree at break point, were observed in the early stage of the aging in water at temperatures above 100 °C, but thereafter both $[\eta]$ and the tensile strength decreased slightly to be held on a certain level. The polymer chain scission took place mainly in the early stage, but thereafter slightly. This was similar as for the aging in 100% RH vapor at 130 °C.

(2) After aging at 130 °C for 192 h, the *p*BAPBDS-based SPI membranes kept the reasonably high mechanical properties. The B/C-SPI membranes kept better mechanical properties; for example, Young's modulus, maximum stress, and elongation degree at break point of 0.9 GPa, 50 MPa, and 14%, respectively.

(3) The decomposition degree of sulfonic acid group in the aging at 130 °C were 0.49% for 96 h and 0.69% for 196 h for the *p*BAPBDS- and BSPB-based SPIs, respectively, indicating the reasonably high hydrolysis stability of sulfonic acid groups. However, the cleavage of sulfopropoxy group took place more easily at 130 °C for the BSPB-based SPIs.

(4) The weight loss and sulfur loss of less than 10% with the aging in water at 130 °C for 96−192 h were observed for the *p*BAPBDS-based SPIs. This was due mainly to the elution of hydrolysis product, which was considered to be the oligomer of NTDA and sulfonated diamine with two or three repeat units of naphthalenic imide−imide structure and naphthalenic imide−acid structure at the chain end(s). The eluted hydrolysis product did not contain the nonsulfonated diamine moieties, suggesting the hydrolysis took place mainly on the imide bonds neighboring sulfonated diamine residues but hardly on the bonds neighboring nonsulfonated ones.

(5) With the aging in 100% RH vapor at 130 °C, the weight loss and sulfur loss were small for the *p*BAPBDS-based SPIs, but rather large for the BSPB-based SPIs because of the elution of sulfopropoxy group.

(6) With the aging at 130 °C, the proton conductivity did not change for the *p*BAPBDS-based SPIs, but for the BSPB-based SPIs it decreased seriously, especially at the lower relative humidities.

(7) As mentioned above, the *p*BAPBDS- and BSPB-based SPI membranes displayed the limited water stability at 130 °C, although being much better than the BSDA-based SPI. Judging from the accelerated water-stability tests, both the *p*BAPBDS- and BSPB-based SPI membranes have the high water stability enough for PEFC and DMFC applications below 80 °C. The *p*BAPBDS-based SPI membranes with further improvement may be applicable to PEFC at temperatures up to 100 °C.

Acknowledgment. This work was financially supported by NEDO (New Energy and Industrial Technology Development): Fuel cell & hydrogen technology development department, "Research and development of polymer electrolyte fuel cells", and by the Venture Business Laboratory of Yamaguchi University, Japan.

References and Notes

(1) Costamagna, P.; Srinivasan, S. *J. Power Sources* **2001**, *102*, 242, 253.
(2) Mehta, V.; Cooper, J. S. *J. Power Sources* **2003**, *114*, 32.
(3) Savadogo, O. *J. New Mater. Electrochem. Syst.* **1998**, *1*, 47.
(4) Mauritz, K. A.; Moore, R. B. *Chem. Rev.* **2004**, *104*, 4535.
(5) Rikukawa, M.; Sanui, K. *Prog. Polym. Sci.* **2000**, *25*, 1463.
(6) Kerres, J. A. *J. Membr. Sci.* **2001**, *185*, 3.
(7) Kreuer, K. D. *J. Membr. Sci.* **2001**, *185*, 29.
(8) Li, Q.; He, R.; Jensen, J. O.; Bjerrum, N. *Chem. Mater.* **2003**, *15*, 4896.
(9) Hickner, M. A.; Ghassemi, H.; Kim, Y. S.; Einsla, B. R.; McGrath, J. E. *Chem. Rev.* **2004**, *145*, 4587.
(10) Faure, S.; Cornet, N.; Gebel, G.; Mercier, R.; Pineri, M.; Sillion, B. In *Proc. 2nd Int. Symp. New Materials for Fuel Cell and Modern Battery Systems*; Savadogo, O., Roberge, P. R., Eds.; Montreal, Canada, July 6−10, 1997; p 818.
(11) Vallejo, E.; Porucelly, G.; Gavach, C.; Mercier, R.; Pineri, M. *J. Membr. Sci.* **1999**, *160*, 127.
(12) Cornet, N.; Diat, O.; Gebel, G.; Jousse, F.; Marsacq, D.; Mercier, R.; Pineri, M. *J. New Mater. Electrochem. Syst.* **2000**, *3*, 33.
(13) Genies, C.; Mercier, R.; Sillion, B.; Cornet, N.; Gebel, G.; Pineri, M. *Polymer* **2001**, *42*, 359.
(14) Besse, S.; Capron, P.; Diat, O.; Gebel, G.; Jousse, F.; Marsacq, D.; Pineri, M.; Marestin, C.; Mercier, R. *J. New Mater. Electrochem. Syst.* **2002**, *5*, 109.
(15) Fang, J.; Guo, X.; Harada, S.; Watari, T.; Tanaka, K.; Kita, H.; Okamoto, K. *Macromolecules* **2002**, *35*, 9022.
(16) Guo, X.; Fang, J.; Watari, T.; Tanaka, K.; Kita, H.; Okamoto, K. *Macromolecules* **2002**, *35*, 6707.
(17) Okamoto, K. *J. Photopolym. Sci. Technol.* **2003**, *16*, 247.
(18) Watari, T.; Fang, J.; Tanaka, K.; Kita, H.; Okamoto, K. *J. Membr. Sci.* **2004**, *230*, 111.
(19) Guo, X.; Fang, J.; Tanaka, K.; Kita, H.; Okamoto, K. *J. Polym. Sci., Part A: Polym. Chem.* **2004**, *42*, 1432.
(20) Guo, X.; Fang, J.; Okamoto, K. *Trans. Mater. Res. Soc. Jpn.* **2004**, *29*, 2579.
(21) Miyatake, K.; Zhou, H.; Uchida, H.; Watanabe, M. *Chem. Commun.* **2003**, 368.
(22) Miyakake, K.; Asano, N.; Watanabe, M. *J. Polym. Sci., Part A: Polym. Chem.* **2003**, *41*, 3901.
(23) Miyatake, K.; Zhou, H.; Matsuo, T.; Uchida, H.; Watanabe, M. *Macromolecules* **2004**, *37*, 4961.
(24) Miyatake, K.; Zhou, H.; Watanabe, M. *Macromolecules* **2004**, *37*, 4956.
(25) Lee, C.; Sundar, S.; Kwon, J.; Han, H. *J. Polym. Sci., Part A: Polym. Chem.* **2004**, *42*, 3612.
(26) Lee, C.; Sundar, S.; Kwon, J.; Han, H. *J. Polym. Sci., Part A: Polym. Chem.* **2004**, *42*, 3621.
(27) Gebel, G.; Gonon, L.; Meyer, G.; Perrot, C. *15th Annual Meeting of NAMS*; Honolulu, HI, June 26−30, 2004; p 110.
(28) Meyer, G.; Gebel, G.; Gonon, L.; Capron, P.; Marscaq, D.; Marestin, C.; Mercier, R. *J. Power Sources*, in press.
(29) Einsla, B. R.; Kim, Y. S.; Hickner, M. A.; Hong, Y.-T.; Hill, M. L.; Pivovar, B. S.; McGrath, J. E. *J. Polym. Sci., Part A: Polym. Chem.* **2004**, *42*, 862.
(30) Einsla, B. R.; Hong, Y.-T.; Kim, Y. S.; Wang, F.; Gunduz, N.; McGrath, J. E. *J. Membr. Sci.* **2005**, *255*, 141.
(31) Yin, Y.; Fang, J.; Cui, Y.; Tanaka, K.; Kita, H.; Okamoto, K. *Polymer* **2003**, *44*, 4509.
(32) Yin, Y.; Fang, J.; Watari, T.; Tanaka, K.; Kita, H.; Okamoto, K. *J. Mater. Chem.* **2004**, *14*, 1062.
(33) Yin, Y.; Yamada, O.; Suto, Y.; Mishima, T.; Tanaka, K.; Kita, H. Okamoto, K. *J. Polym. Sci., Part A: Polym. Chem.* **2005**, *43*, 1545.
(34) Asano, N.; Miyatake, K.; Watanabe, M. *Chem. Mater.* **2004**, *16*, 2841.

(35) Yin, Y.; Hayashi, S.; Yamada, O.; Kita, H.; Okamoto, K. *Macromol. Rapid Commun.* **2005**, *26*, 696.
(36) Genies, C.; Mercier, R.; Sillion, B.; Petiaud, R.; Cornet, N.; Gebel, G.; Pineri, M. *Polymer* **2001**, *42*, 5097.
(37) Yamada, O.; Yin, Y.; Fukuda, T.; Tanaka, K.; Kita, H.; Okamoto, K. *45th Battery Symp. Jpn.* **2004**, *27*, 666.

MA0523769